

Contents lists available at [ScienceDirect](http://ScienceDirect)

## Physics Letters B

[www.elsevier.com/locate/physletb](http://www.elsevier.com/locate/physletb)

## Pygmy Quadrupole Resonance in skin nuclei

N. Tsoneva<sup>a,b,\*</sup>, H. Lenske<sup>a</sup><sup>a</sup> Institut für Theoretische Physik, Universität Gießen, Heinrich-Buff-Ring 16, D-35392 Gießen, Germany<sup>b</sup> Institute for Nuclear Research and Nuclear Energy, 1784 Sofia, Bulgaria

## ARTICLE INFO

## Article history:

Received 29 October 2009

Received in revised form 14 August 2010

Accepted 26 October 2010

Available online 6 November 2010

Editor: J.-P. Blaizot

## Keywords:

Nuclear models

Nuclear skins

Giant resonances

Pygmy resonances

## ABSTRACT

The electric quadrupole response is investigated theoretically by HFB and QPM calculations along the Sn isotopic chain with special emphasis on excitations above the first collective state and below the particle threshold. Depending on the asymmetry, additional quadrupole strength clustering as a group of states similar to the known Pygmy Dipole Resonance is found. The spectral distributions, electric quadrupole response functions and transition densities of low-energy quadrupole states show special features being compatible with oscillations of neutron or proton skins against the nuclear core.

© 2010 Elsevier B.V. Open access under [CC BY license](http://creativecommons.org/licenses/by/3.0/).

## 1. Introduction

One of the most interesting results of nuclear structure physics in recent years was the discovery of a new dipole mode at energies below and close to the particle emission threshold [1], observed in stable and unstable nuclei with charge asymmetry  $N/Z > 1$ . Typically, that strength is found as a bunching of discrete  $1^-$  states with very similar spectroscopic features. This extra dipole strength could not be explained as part of the low-energy tail of the Giant Dipole Resonance (GDR) [2] and the mode was named Pygmy Dipole Resonance (PDR). The PDR is of high current interest and its properties are investigated by a large number of theoretical and experimental groups [2–16]. Theoretically, there is agreement that the PDR is an isospin-mixed mode, connected to excitations of the surface layer of excess matter in  $N \neq Z$  nuclei, e.g. neutrons in a  $N > Z$  nucleus. The PDR states indicate a new mode of nuclear excitation corresponding to a vibrational motion of the nuclear skin against the core [9–16].

An obvious question, arising immediately in this context, is to what extent the presence of a neutron or proton skin will affect excitations of other multiplicities and *vice versa*. Promising candidates are low-energy  $2^+$  states, especially those in excess of the spectral distributions known from stable nuclei. Multipole response functions in neutron-rich nuclei have been studied the-

oretically before, e.g. Refs. [17–22]. In particular, in Refs. [21,22] spectral distributions of  $0^+$ ,  $1^-$  and  $2^+$  excitations in the Ca, Ni, and Sn isotopes far beyond stability have been investigated in a self-consistent Skyrme Hartree-Fock-Bogolubov (HFB) and Quasi-particle Random Phase Approximation (QRPA) approach. Similar results were presented in Hartree-Fock (HF) plus Random Phase Approximation (RPA) calculation regarding  $^{28}\text{O}$  [19,20] and in our recent HFB plus QRPA calculations in  $^{120}\text{Sn}$  [23] where a concentration of low-energy electric quadrupole strength, located below the Isoscalar Giant Quadrupole Resonance (ISGQR) [24] was found. A related, but somewhat different aspect is considered in Ref. [25] where isoscalar and isovector quadrupole modes in the vicinity of the giant resonances in neutron-rich nuclei are discussed.

In this Letter we investigate low-energy quadrupole excitations in charge-asymmetric nuclei. We are interested especially in the question to what extent these excitations can serve as signatures for dynamical processes related to isospin asymmetry in  $\beta$ -unstable skin nuclei. We choose the Sn isotopic chain as a suitable test case.

## 2. Theoretical model

Our approach is based on a phenomenological energy-density functional (EDF) [3,9,26]. The excited states are calculated with QRPA theory, using the multi-phonon description of the Quasi-particle-Phonon model (QPM) [27]. Their unique spectroscopic properties are revealed in analysis of transition densities and spectral functions. While in [21,22] the overall features of multipole response functions in nuclei far off stability were considered, here

\* Corresponding author at: Institut für Theoretische Physik, Universität Gießen, Heinrich-Buff-Ring 16, D-35392 Gießen, Germany.

E-mail address: [tsoneva@theo.physik.uni-giessen.de](mailto:tsoneva@theo.physik.uni-giessen.de) (N. Tsoneva).

our interest is on a more focused question, namely on studying the dependence of low-energy quadrupole strengths on the neutron-to-proton ratio and their interpretation on a macroscopic level. The microscopic results indicate an interesting relation to the nuclear collective degrees of freedom: these quadrupole excitations may be understood as a new kind of nuclear surface vibrations related to dynamical variations of the diffusivity, hence reflecting changes in the surface tension.

The building blocks of the model are given by the quasiparticle states obtained from a HFB description of the nuclear ground states and coherent superpositions of two-quasiparticle (2QP) states treated by QRPA theory. A detailed description of the approach is found in [3,9], here we give only a brief overview. The approach is based on the Hamiltonian

$$H = H_{MF} + H_{res}. \quad (2.1)$$

The mean-field part  $H_{MF}$  defines the single particle properties and, as such, accounts for the ground state dynamics, including potentials and pairing interactions for protons and neutrons, respectively. That part is related to an EDF [3,9] constructed such that also dynamical effects beyond mean-field can be taken into account. That goal is achieved in practice by using fully microscopic HFB potentials and pairing fields as input but performing a second step variation with scaled auxiliary potentials and pairing fields readjusted in a self-consistent manner such that nuclear binding energies and other ground state properties of relevance are closely reproduced.

The residual interactions contained in  $H_{res}$  are treated separately. After having derived the ground state single quasiparticle spectra and wave functions the nuclear excited states are described by QRPA phonons of various multipolarities. Following the notation of [27], the state operators are defined as a combination of 2QP creation  $A^+$  and annihilation  $A^-$  operators, respectively:

$$Q_{\lambda\mu}^+ = \frac{1}{2} \sum_{jj'} (\psi_{jj'}^{\lambda i} A_{\lambda\mu}^+(jj') - \varphi_{jj'}^{\lambda i} \tilde{A}_{\lambda\mu}(jj')) \quad (2.2)$$

where,  $j \equiv (nljm\tau)$  is a single-particle proton or neutron state;  $\psi_{j_1 j_2}^{\lambda i}$  and  $\varphi_{j_1 j_2}^{\lambda i}$  are the configuration time-forward and time-backward amplitudes [27], respectively. The operators are coupled to total angular momentum  $\lambda$  with projection  $\mu$ .

The phonons obey the QRPA equation of motion

$$[H, Q_\alpha^+] = E_\alpha Q_\alpha^+, \quad (2.3)$$

accounting now also for the residual interactions in the particle-hole ( $p$ - $h$ ) and the particle-particle ( $p$ - $p$ ) channels, respectively. By solving the eigenvalue problem, Eq. (2.3), we obtain the phonon excitation energies  $E_\alpha$  and the state vectors, Eq. (2.2).

In the QRPA calculations we use residual interactions given by

$$H_{res} = H_M^{ph} + H_{SM}^{ph} + H_M^{pp}. \quad (2.4)$$

In this work, we do not attempt a fully self-consistent derivation of  $H_{res}$  but follow the empirical approach of the QPM [27, 37–39]. Hence, we use separable multipole-multipole  $H_M^{ph}$  and spin-multipole  $H_{SM}^{ph}$  interactions both of isoscalar and isovector type in the  $p$ - $h$  and multipole pairing  $H_M^{pp}$  in the  $p$ - $p$  channels, respectively [37]. However, since the  $Z = 50$  shell closure is rather persistent over the full mass range, in practice only the neutrons are affected by the  $p$ - $p$  interactions. For the definition of the quadrupole-quadrupole interactions and the determination of the coupling strength parameters of the  $p$ - $h$  and  $p$ - $p$  channels we follow a procedure commonly used in the QPM model [38] – they are fitted to energies and transition probabilities of the first  $2_1^+$  states (except for the case of  $^{104}\text{Sn}$  which is explained

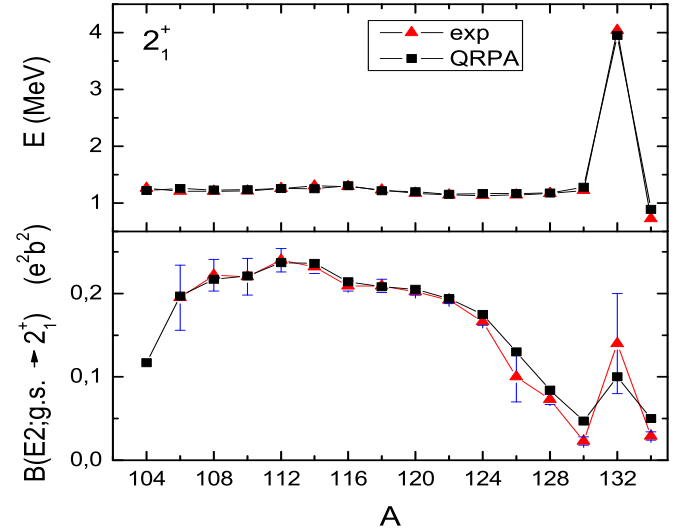


Fig. 1. QRPA calculations of the energies (upper panel) and transition strengths (lower panel) of the first  $2_1^+$  states in  $^{104-134}\text{Sn}$  compared to experimental data [28–36].

below). In addition, we only mention the interesting observation that in the nuclei considered here the isoscalar constant  $\kappa_0^{(2)}$  of the quadrupole-quadrupole  $p$ - $h$  interaction is rather independent of the nuclear mass with only slight variations, typically in the order of 1% between neighboring stable nuclei and less than 5% outside the valley of stability. This allows safe extrapolations into the hitherto unexplored regions toward  $^{100}\text{Sn}$  and beyond  $^{132}\text{Sn}$ .

### 3. Quadrupole excitations in Sn isotopes

#### 3.1. The quadrupole response functions

We first discuss the properties of the conventionally known parts of the quadrupole spectrum. These considerations serve also as tests before focusing on new features of the quadrupole spectrum. The fitted QRPA results for energies and  $B(E2)$  transition probabilities of the  $[2_1^+]_{QRPA}$  state are displayed and compared to data [31–33] in Fig. 1. It is seen that the QRPA model parameters are reliably determined. The excitation energies are remarkably stable over the mass range, except at the shell closure at  $A = 132$ . Also the transition strengths vary only mildly in a narrow band for most of the isotopes but decreasing when  $^{132}\text{Sn}$  is approached. Adjusting the model parameters in  $^{104}\text{Sn}$  to the experimental energy of the  $2_1^+$  state we find  $E_{2_1^+}^* = 2.221$  MeV [28] and  $B(E2; \text{g.s.} \rightarrow [2_1^+]_{QRPA}) = 0.10e^2b^2$ . The extrapolation to  $^{104}\text{Sn}$  result in changes of the model parameters on a level of a few percent. Thus, we reproduce the experimentally observed trend of decreasing  $B(E2)$  values toward  $^{100}\text{Sn}$  which is also found in shell model calculations [31].

For understanding the evolution of shell structures far from stability, the region around the double magic nucleus  $^{132}\text{Sn}$  is of particular interest. The restoration of the  $N = 82$  neutron-shell gap was recently confirmed by high-precision mass measurements [40]. From a systematic study of  $2_1^+$  states [41], the product of transition strength and excitation energy was found to be almost constant, i.e.  $B(E2; \text{g.s.} \rightarrow 2_1^+) \approx 1/E(2_1^+)$ . First of all, this means that the contributions of the  $2_1^+$  states to the electromagnetic energy weighted sum rule (EWSR) is within narrow limits a constant. The electromagnetic EWSR, on the other hand, is known to be expressible in closed form by the ground state expectation value of the double commutator of the electric quadrupole transition oper-



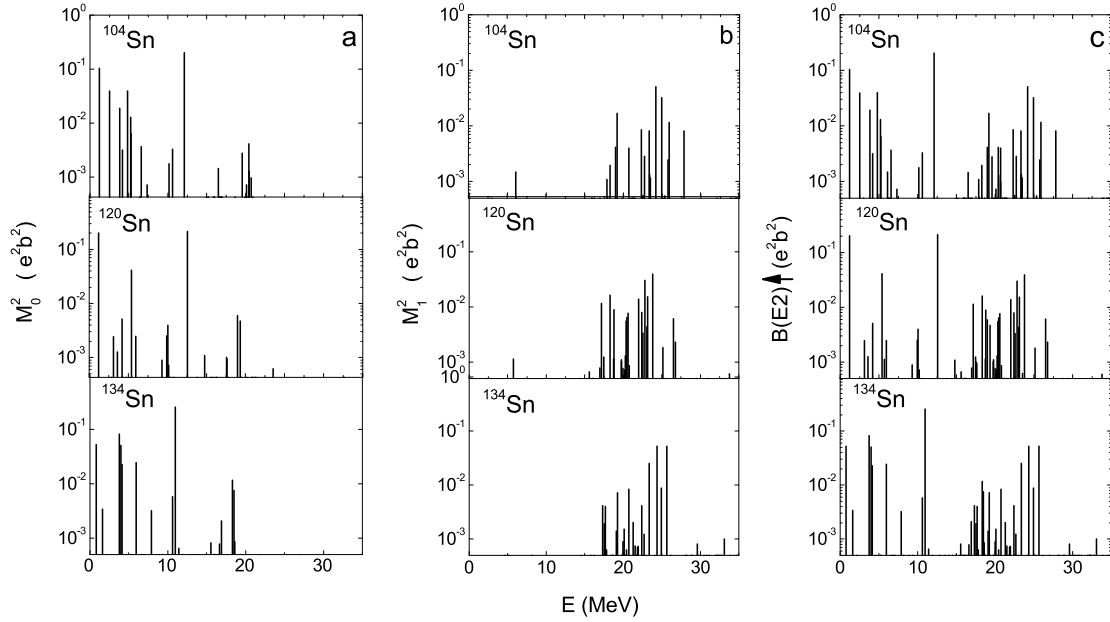


**Fig. 4.** QRPA results for the isoscalar (a) and isovector (b) partial contributions, respectively, and the total electric quadrupole strengths (c) in the Sn isotopes.

tal  $B(E2)$  values toward  $A \approx 120$ . This is related to the diminishing contribution of the protons, which are coupled directly by their physical charge to the electromagnetic field. The increase of the  $B(E2)$  strength in the mass region  $A \geq 120$  is due to the increasing neutron contributions which couple indirectly by recoil effects and related effective charges to the electromagnetic field, thus reflecting a particular many-body effect. This increasing strength is mainly related to the mass dependence of the 2QP transition matrix elements and the decrease of the neutron separation energies toward  $^{132}\text{Sn}$ . A simple estimation from the asymptotics of the radial wave functions shows that  $B(E2) \approx 1/|\epsilon_b|^2$  thus indicating the strong increase of the  $B(E2)$  with decreasing binding energy  $\epsilon_b$ .

Investigations of the relative signs of proton and neutron amplitudes of the  $[2_2^+]_{QRPA}$  and  $[2_3^+]_{QRPA}$  states indicate that they are of isoscalar character for tin isotopes with larger masses  $A \geq 126$  while they are of mixed symmetry for the lighter ones. Nevertheless, these mixed symmetry states have to be distinguished from low-energy quadrupole mixed-symmetry states known as scissors modes [44]. A genuine signature of the scissors mode in near-vibrational nuclei is based on the strong M1 transition (of the order of  $1\mu_N^2$ ) to the first symmetric  $2_1^+$  state [45]. One- and two-phonon mixed-symmetry states in  $N = 80$  and  $N = 84$  isotones in a close connection with the scissors mode have been investigated in standard QPM in [46].

In our case, the multiphonon calculations lead to rather small M1 strength of the order of  $10^{-2}\mu_N^2$ .

Taking together our QRPA and QPM observations we conclude that low-energy quadrupole excitations with a dominant neutron content could belong to a new quadrupole mode related to a neutron surface vibrations. A supporting argument in this direction could be a possible connection between  $B(E2)$  transition rates of these states and the neutron excess. Such example are the almost pure neutron  $[2_2^+]_{QRPA}$  and  $[2_3^+]_{QRPA}$  states in Sn isotopes with  $A \geq 120$  as it is seen in Fig. 2.

Theoretical results of  $B(E2)$  spectral transition strength distributions in  $^{104,120,134}\text{Sn}$  isotopes are presented in Fig. 4. A sizable increase of  $B(E2)$  strength at  $E_x \approx 2\text{--}4$  MeV is observed for the heaviest tin isotopes –  $^{130}\text{Sn}$  and  $^{134}\text{Sn}$  – studied here.

In the lighter tin isotopes the reduced neutron number decreases the collectivity of the  $[2_1^+]_{QRPA}$  state which becomes non-

collective in  $^{104}\text{Sn}$ . At the same time the proton contribution to the  $B(E2)$  strength located in the energy range 2–4 MeV increases toward  $^{104}\text{Sn}$  and brings to more intensive proton quadrupole excitations in  $^{104}\text{Sn}$  there (see Figs. 2 and 4c). Consequently, the  $^{104}\text{Sn}$  nucleus appears to be an opposing case where a change from a neutron to a proton skin occurs. The clustering of quadrupole states at low-energies shows a pattern similar to the PDR phenomenon. Therefore, we may consider the spectral distribution a neutron Pygmy Quadrupole Resonance (PQR). Correspondingly, the PQR changes character as well from a dominance of neutron to proton excitations, respectively.

In order to study the isospin effects explicitly, we consider the multipole matrix elements  $M_I(\lambda\mu)$  for  $\lambda = 2$  defined by:

$$M_I(2^+) \approx \langle 2^+ | \sum_k r_k^2 Y_{2\mu}(\Omega_k) (\tau_3)^I | \text{g.s.} \rangle, \quad (3.2)$$

where  $I = 0, 1$  indicates the isoscalar and isovector transition operators.

The distributions of the isoscalar  $M_0$  and isovector  $M_1$  quadrupole strengths in  $^{104\text{--}134}\text{Sn}$  up 35 MeV are presented in Fig. 4a, b, respectively.

### 3.2. Quadrupole transition densities

The spatial pattern of the transitions is contained in the transition densities from the ground state  $|0\rangle$  to an excited state  $Q_{\lambda\mu}^+|0\rangle$

$$\rho_{\lambda i}^I = \langle Q_{\lambda\mu}^+ | \hat{\rho}_{\lambda i}^I | 0 \rangle, \quad (3.3)$$

where  $\rho_{\lambda i}^I$  is isoscalar ( $I = 0$ ) or isovector ( $I = 1$ ) one-body density matrix.

In  $^{106\text{--}134}\text{Sn}$  most of the quadrupole states below the particle emission threshold are of isoscalar character. However, some mixed symmetry configurations are also observed in this region, as seen in Fig. 5. At lower energies,  $E_x = 2\text{--}4$  MeV and  $E_x = 0.8\text{--}3.7$  MeV in  $^{120}\text{Sn}$  and  $^{134}\text{Sn}$ , respectively, the main part of the oscillations is coming from less strongly bound neutrons, forming a skin-like surface layer [9], located predominantly at the nuclear periphery, extending to radii up to  $r \approx 10$  fm in  $^{120}\text{Sn}$  and up to  $r \approx 20$  in

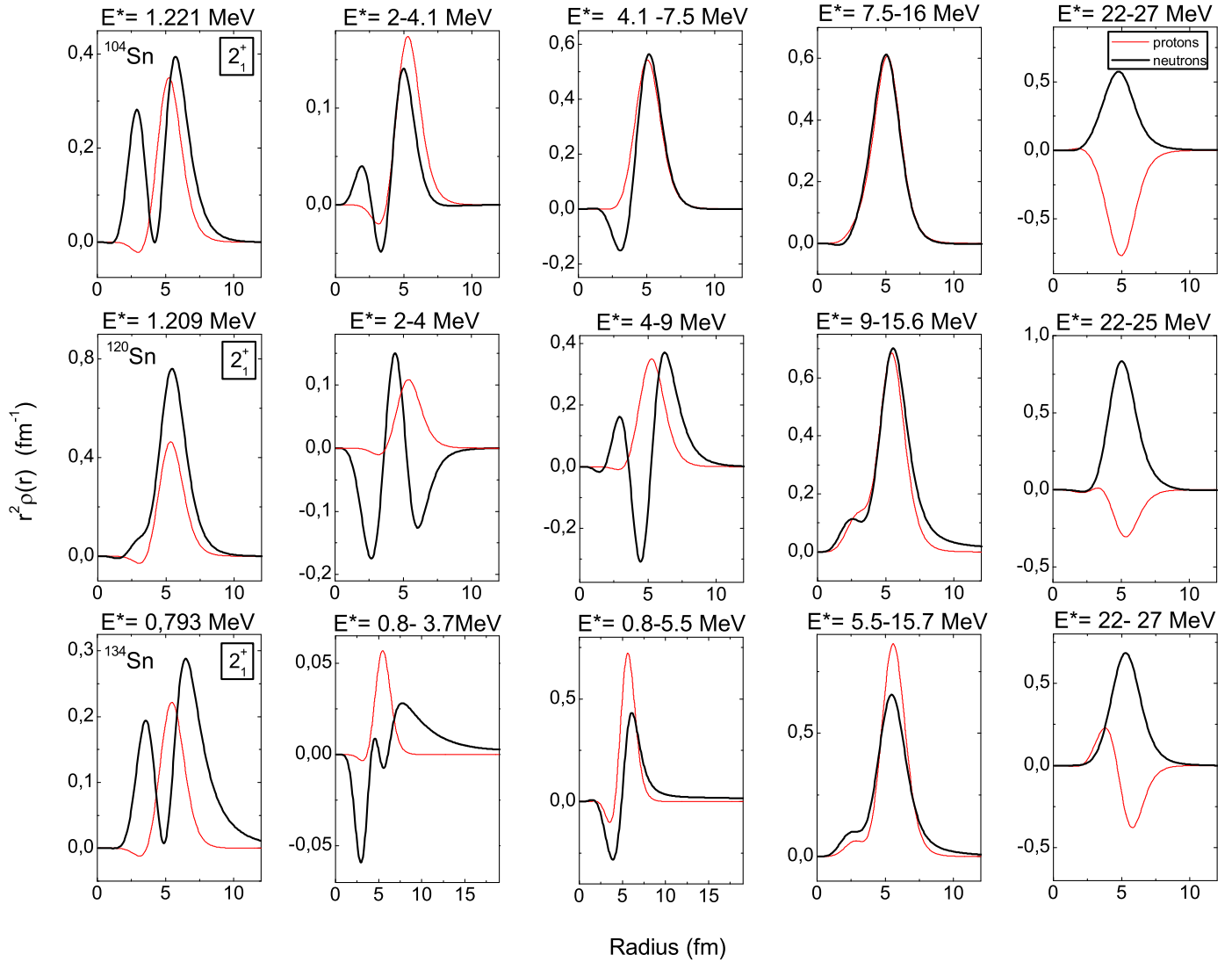


Fig. 5. QRPA proton (dash line) and neutron (solid line) quadrupole transition densities summed over  $[2^+]_{QRPA}$  excited states in a given energy region (indicated over every plot) in  $^{104,120,134}\text{Sn}$  isotopes.

$^{134}\text{Sn}$ . At the same time we find a very small proton contribution in this space region.

For the double-magic  $^{132}\text{Sn}$  the first QRPA  $2^+$  ( $E_x = 3.9$  MeV) and the second QRPA  $2^+$  ( $E_x = 5.3$  MeV) states exhibit properties similar to the neutron states discussed in the other tin isotopes in the same energy range. These states incorporate strength related to oscillations of neutrons at the surface region. The second  $2^+$  state includes an additional component resembling the oscillation pattern of an isoscalar excitation as e.g. as in the ISGQR.

As seen in Fig. 5, the proton and neutron transition densities of the low-energy states change their behavior when approaching  $^{104}\text{Sn}$ . The proton components increase and finally dominate in  $^{104}\text{Sn}$ . These features indicate the change from a neutron PQR to a proton PQR in the isotopes lighter than  $^{104}\text{Sn}$ , similarly to the PDR case [9,11,15].

With the increase of the excitation energy  $E_x$  toward the particle separation threshold, the quadrupole states become more collective with a larger admixture of isovector components to the state vectors. Nevertheless, some isospin effects are still present up to the particle emission threshold (even strongly hindered). In this case, in  $^{106-130}\text{Sn}$  isotopes we observe more isovector type of oscillations inside the nucleus while at the surface neutrons domi-

nate. These higher-lying states could not be related directly to skin effects as they collect a lot of strength, which is of the same order as for the collective  $2^+$  and the IS(V)GQRs. The contribution of nucleons from the nuclear interior at these intermediate excitation energies is significant. At the same time the role of the isospin effects, in particular the neutron skin for energies close to the threshold has to be further investigated. The last two plots in every row of Fig. 5 show the proton and neutron transition densities of the ISGQR and IVGQR, respectively.

Overall, the transition densities show an interesting dependence on the excitation energy: in all nuclei the isoscalar character of the lowest  $2^+$  state and of the GQR is evident from the in-phase behavior of proton and neutron components, while proton and neutron transition densities carry opposite phases in the isovector GQR region. Together with the almost identical radial shapes these results reproduce perfectly well the generally accepted rules for collective quadrupole states. They are well interpreted as surface and volume oscillations of a liquid drop [47]. However, the transition densities related to the additional quadrupole states which may be considered as PQR excitations are not following any of the known rules but are showing quite unusual properties. As seen from Fig. 5, the proton components continue to behave like vibra-



tional variations of the nuclear density radius while the neutron transition densities develop a rather different nodal pattern. The nodal structures correspond to processes where a (tiny) portion of nuclear matter is shuffled around the nuclear radius, leaving the latter almost unaffected, as indicated by the radial node occurring at or close to the nuclear half density radius,  $R \sim 5$  fm.

In a liquid drop picture, these features can be interpreted as vibrational excitations of the nuclear surface given by a superposition of variations in position and diffuseness of the surface. The latter mode was already anticipated by Bohr and Mottelson [48], although hitherto experimentally never verified, at least not in stable nuclei. Our results give evidence that such modes may indeed exist as low-energy excitations in charge-asymmetric nuclei.

In fact, in a collective model approach we may consider not only the nuclear radius  $R$  but also the diffusivity  $a$  as a dynamical quantity. Hence, in addition to the well-known representation of the nuclear radius  $R = R_A f(\Omega, \alpha^\dagger)$  in terms of the collective multipole amplitudes  $\alpha_{\lambda\mu}^\dagger$  [48] we may introduce

$$a_q = c_q \sum_{\lambda, \mu \geq 2} Y_{\lambda\mu}^*(\Omega) \beta_{\lambda\mu}^\dagger \quad (3.4)$$

describing the dynamical variation of the diffusivity of proton ( $q = p$ ) and neutron ( $q = n$ ) densities, respectively, around the equilibrium value  $c_q$  with amplitudes determined by the respective mode operators  $\beta_{\lambda\mu}^\dagger$ . For an illustration we consider a nuclear density of Fermi function shape. Expanding up to first order in the vibrational amplitudes, the generalized collective multipole transition densities are found to have the radial form factors

$$\rho_{q\lambda}(r) = \rho_{0q} \left( a_{q\lambda} + b_{q\lambda} \frac{r - R_A}{R_A} \right) f'(x) \quad (3.5)$$

where  $f'(x)$  denotes the derivative of a Fermi function  $f(x) = 1/(1 + e^x)$  with respect to the argument  $x = \frac{r - R_A}{c_q}$ . The amplitudes  $a_{q\lambda}$  and  $b_{q\lambda}$  denote the surface and diffusivity vibrations. While the first part describes the well established surface vibrations due to variations of the nuclear radius, i.e. the slight motions of the nuclear surface as a whole, the second component keeps the radius fixed but moves the surface in a kind of tilting mode by variation of the diffusivity. Explicit calculations show that the transition matrix elements related this tilting mode increase rapidly with the diffusivity  $c_q$ , similar to the dependencies found in the microscopic calculations.

This interpretation is supported by a result of Pethick and Ravenhall [49] who derived a relation connecting the thickness of the nuclear skin to the surface tension. According to their result, the surface tension decreases with increasing neutron excess. However, they did not consider diffusivity vibrations which will lead to additional contributions. Now, as mentioned, the shapes of the PQR neutron transition densities are compatible with a reordering of neutron skin matter around the nuclear surface, described the best as an oscillatory alteration of the surface thickness and, consequently, the surface tension.

#### 4. Conclusions

Quadrupole states were investigated in  $^{104-134}\text{Sn}$  nuclei up to excitation energies of 35 MeV. For the double-magic  $^{132}\text{Sn}$  an increase of the  $B(E2; \text{g.s.} \rightarrow 2_1^+)$  compared to the neighbor  $^{130}\text{Sn}$  and  $^{134}\text{Sn}$  is observed and explained. For  $^{104}\text{Sn}$ , the  $B(E2)$  transition probability of the first  $2^+$  state is predicted and its spectroscopic properties are determined. From the analysis of isoscalar and isovector electric quadrupole strength distributions the nature of the quadrupole states is investigated and a separation be-

tween collective isoscalar, isovector and low-energy mixed symmetry states is achieved. The spectral distribution of the low-energy states in  $^{104-134}\text{Sn}$  clustered in a confined energy region may be considered as a PQR. An increase of the low-energy  $B(E2)$  strength, which is due mainly to neutron excitations, is found toward  $^{134}\text{Sn}$ .

Our calculations of M1 and E2 transitions of low-energy mixed symmetry  $2_2^+$  and  $2_3^+$  in tins with  $A < 126$  indicate that these states are of a genuine character, different from the known scissors mode.

An especially interesting aspect is the close relation of the PQR excitations to the shell structure as discussed in connection with Fig. 3. Apparently, the appearance of the PQR states is depending on reorientation excitations within a sub-shell. The best evidence for this feature is the disappearance of the PQR component in the double magic  $^{132}\text{Sn}$  nucleus. Thus, the PQR states are containing subtle information on the valence shells and their evolution with the nuclear mass number. In addition, the correlation of the PQR transition strength with the neutron or proton skin thickness manifests itself via a transition from a neutron PQR to a proton PQR in  $^{104}\text{Sn}$ , the mass region where the neutron skin reverses into a proton skin.

By means of quadrupole transition densities the nature of the PQR is clarified. In general, the PQR resembles the properties of the PDR and could be related to skin oscillations of one type of nucleons. Even though, with the increase of the collectivity of the quadrupole excitations the reliable distinction of the pure skin neutron (proton) quadrupole oscillations seems to be a difficult task, especially for nuclei with small or moderate neutron excess. In this respect, nuclei with larger isospin asymmetry beyond  $^{130}\text{Sn}$  will be a good candidates for experimentally explorations.

#### Acknowledgements

The work is supported by DFG grant Le439/7 and BMBF project 06G19109.

#### References

- [1] U. Kneissl, N. Pietralla, A. Zilges, J. Phys. G 32 (2006) R217.
- [2] R. Schwengner, et al., Phys. Rev. C 78 (2008) 064314.
- [3] N. Tsoneva, H. Lenske, Ch. Stoyanov, Phys. Lett. B 586 (2004) 213.
- [4] K. Govaert, et al., Phys. Rev. C 57 (1998) 2229.
- [5] B. Özel, et al., Nucl. Phys. A 778 (2007) 385.
- [6] N. Ryezayeva, et al., Phys. Rev. Lett. 89 (2002) 272502.
- [7] S. Volz, et al., Nucl. Phys. A 779 (2006) 1.
- [8] P. Adrich, et al., Phys. Rev. Lett. 95 (2005) 132501.
- [9] N. Tsoneva, H. Lenske, Phys. Rev. C 77 (2008) 024321, and references therein.
- [10] N. Paar, et al., Phys. Rev. C 67 (2003) 034312.
- [11] N. Paar, et al., Phys. Lett. B 624 (2005) 195.
- [12] D. Sarchi, P.F. Bortignon, G. Colò, Phys. Lett. B 601 (2004) 27.
- [13] S. Kamedzhiev, J. Speth, G. Terentychny, Phys. Rep. 393 (2004) 1.
- [14] E. Litvinova, P. Ring, D. Vretenar, Phys. Lett. B 647 (2007) 111.
- [15] C. Barbieri, et al., Phys. Rev. C 77 (2008) 024304.
- [16] A. Tonchev, et al., Phys. Rev. Lett. 104 (2010) 072501.
- [17] P. Van Isacker, M.A. Nagarajan, D.D. Warner, Phys. Rev. C 45 (1992) R13.
- [18] D.D. Warner, P. Van Isacker, Phys. Lett. B 395 (1997) 145.
- [19] M. Yokoyama, T. Otsuka, N. Fukunishi, Phys. Rev. C 52 (1995) 1122.
- [20] M. Yokoyama, T. Otsuka, N. Fukunishi, Nucl. Phys. A 599 (1996) 367c.
- [21] J. Terasaki, J. Engel, Phys. Rev. C 74 (2006) 044301.
- [22] J. Terasaki, J. Engel, Phys. Rev. C 74 (2007) 044320.
- [23] N. Tsoneva, H. Lenske, AIP Conf. Proc. 1090 (2009) 409.
- [24] M.N. Harakeh, A. van der Woude, Giant Resonances, Clarendon Press, Oxford, 2001.
- [25] F. Catara, et al., Nucl. Phys. A 614 (1997) 86.
- [26] F. Hofmann, H. Lenske, Phys. Rev. C 57 (1998) 2281.
- [27] V.G. Soloviev, Theory of Complex Nuclei, Pergamon Press, Oxford, 1976.
- [28] J. Blacot, Nucl. Data Sheets 108 (2007) 20163.
- [29] C. Vaman, et al., Phys. Rev. Lett. 99 (2007) 162501.
- [30] A. Banu, et al., Phys. Rev. C 72 (2005) 061305.
- [31] A. Ekström, et al., Phys. Rev. Lett. 101 (2008) 012502.
- [32] J. Cedercäll, et al., Phys. Rev. Lett. 98 (2007) 172501.

- [33] J.N. Orce, et al., Phys. Rev. C 77 (2008) 029902 (Erratum).
- [34] P. Doornenbal, et al., Phys. Rev. C 78 (2008) 031303(R).
- [35] S. Raman, C.W. Nestor, P. Tikkanen, At. Data Nucl. Data Tables 78 (2001) 1.
- [36] D.C. Radford, et al., Nucl. Phys. A 746 (2004) 83c.
- [37] V.G. Soloviev, Theory of Atomic Nuclei: Quasiparticles and Phonons, Inst. of Phys. Publ., Bristol, 1992.
- [38] A. Vdovin, V.G. Soloviev, Physics of Elementary Particles and Atomic Nuclei 14 (2) (1983) 237.
- [39] V.Yu. Ponomarev, Physics of Elementary Particles and Atomic Nuclei (PEPAN) 29 (1998) 1354, Part 6.
- [40] M. Dworschak, et al., Phys. Rev. Lett. 100 (2008) 172501.
- [41] J. Terasaki, et al., Phys. Rev. C 66 (2002) 054313, and references therein.
- [42] H. Feshbach, A. de Shalit, Theoretical Nuclear Physics, vol. 1, Nuclear Structure, Wiley, 1974.
- [43] A.P. Severyukhin, V.V. Voronov, N. Van Giai, Phys. Rev. C 77 (2008) 024322.
- [44] N. Lo Iudice, F. Palumbo, Phys. Rev. Lett. 41 (1978) 1532.
- [45] N. Pietralla, P. von Brentano, A.F. Lisetskiy, Prog. Part. Nucl. Phys. 60 (2008) 225.
- [46] N. Lo Iudice, Ch. Stoyanov, Phys. Rev. C 65 (2002) 064304, and references therein.
- [47] D.J. Rowe, Nuclear Collective Motion: Models and Theory, Methuen, London, 1970.
- [48] A. Bohr, B. Mottelson, Nuclear Structure: Nuclear Deformations, vol. 2, W.A. Benjamin, Boston, 1975, p. 343.
- [49] C.J. Pethick, D.G. Ravenhall, Nucl. Phys. A 606 (1996) 173.